

Title	Synchronisation vs. resonance: Isolated resonances in damped nonlinear oscillators
Authors	Marchionne, Arianna;Ditlevsen, Peter;Wieczorek, Sebastian
Publication date	2018-06-01
Original Citation	Marchionne, A., Ditlevsen, P. and Wieczorek, S. (2018) 'Synchronisation vs. resonance: Isolated resonances in damped nonlinear oscillators', Physica D: Nonlinear Phenomena, In Press. doi: 10.1016/j.physd.2018.05.004
Type of publication	Article (peer-reviewed)
Link to publisher's version	<a href="https://www.sciencedirect.com/science/article/pii/S0167278917302865">https://www.sciencedirect.com/science/article/pii/S0167278917302865</a> - 10.1016/j.physd.2018.05.004
Rights	© 2018 Elsevier B.V. All rights reserved. This manuscript version is made available under the CC-BY-NC-ND 4.0 license. - <a href="https://creativecommons.org/licenses/by-nc-nd/4.0/">https://creativecommons.org/licenses/by-nc-nd/4.0/</a>
Download date	2024-05-05 01:47:56
Item downloaded from	<a href="https://hdl.handle.net/10468/6251">https://hdl.handle.net/10468/6251</a>



# UCC

**University College Cork, Ireland**  
 Coláiste na hOllscoile Corcaigh

## Accepted Manuscript

Synchronisation vs. resonance: Isolated resonances in damped nonlinear oscillators

Arianna Marchionne, Peter Ditlevsen, Sebastian Wieczorek

PII: S0167-2789(17)30286-5  
DOI: <https://doi.org/10.1016/j.physd.2018.05.004>  
Reference: PHYSD 32024

To appear in: *Physica D*

Received date: 22 May 2017  
Revised date: 16 February 2018  
Accepted date: 25 May 2018

Please cite this article as: A. Marchionne, P. Ditlevsen, S. Wieczorek, Synchronisation vs. resonance: Isolated resonances in damped nonlinear oscillators, *Physica D* (2018), <https://doi.org/10.1016/j.physd.2018.05.004>

This is a PDF file of an unedited manuscript that has been accepted for publication. As a service to our customers we are providing this early version of the manuscript. The manuscript will undergo copyediting, typesetting, and review of the resulting proof before it is published in its final form. Please note that during the production process errors may be discovered which could affect the content, and all legal disclaimers that apply to the journal pertain.



Arianna Marchionne and Peter Ditlevsen  
*Niels Bohr Institute, University of Copenhagen, Denmark*

Sebastian Wieczorek  
*Department of Applied Mathematics, University College Cork, Ireland*  
 (Dated: May 30, 2018)

We describe differences between synchronisation and resonance, and analyse different types of nonlinear resonances in a weakly damped Duffing oscillator using bifurcation theory techniques. In addition to previously reported (i) odd subharmonic resonances found on the primary branch of symmetric periodic solutions with the forcing frequency and (ii) even subharmonic resonances due to symmetry-broken periodic solutions that bifurcate off the primary branch and also oscillate at the forcing frequency, we uncover (iii) novel resonance type due to isolas of periodic solutions that are not connected to the primary branch. These occur between odd and even resonances, oscillate at a fraction of the forcing frequency, and give rise to a complicated resonance ‘curve’ with disconnected elements and high degree of multistability.

We use bifurcation continuation to compute resonance tongues in the plane of the forcing frequency vs. the forcing amplitude for different but fixed values of the damping rate. Our analysis shows that identified here isolated resonances explain the intriguing “intermingled tongues” that were observed for weak damping and misinterpreted as (synchronisation) Arnold tongues in [Phys. Rev. E 57, 1554 (1998)]. What is more, isolated resonances link “intermingled tongues” to a seemingly unrelated phenomenon of “bifurcation superstructure” described for moderate damping in [Phys. Lett. A 107, 351 (1985)].

## INTRODUCTION

Many complex systems in the natural world and technology show oscillatory behaviour, either as self-sustained oscillations, or as response to external forcing. Even though the description of the detailed dynamics is often incomplete, such systems can be modelled and understood in terms of low-dimensional nonlinear oscillators that capture the dominating degrees of freedom. Throughout the paper, we refer to two oscillator types:

- *damped oscillators*: linear or nonlinear dissipative dynamical systems that exhibit oscillations whose amplitude decays to zero over time (e.g. stable equilibrium with a pair of complex conjugate eigenvalues), and
- *dissipative self-sustained oscillators*: nonlinear dissipative dynamical systems that exhibit self-sustained oscillations (e.g. a stable limit cycle).

When an oscillator is subject to external periodic forcing, two widely studied phenomena are at play, depending on the behaviour of the unforced system. Firstly, a linear (harmonic) damped oscillator exhibits increased amplitude of oscillations when forced near its natural frequency. The situation becomes surprisingly more complex in ubiquitous nonlinear damped oscillators, which exhibit increased amplitude of oscillations together with bistability (or even multistability) near several subharmonic forcing frequencies. This is the phenomenon of resonance [1, 2]. Secondly, when dissipative self-sustained oscillators are subject to external periodic forcing, or coupled to one another, they may lock their frequencies at

different ratios. This is the phenomenon of synchronisation, which is even more complicated than nonlinear resonances [2].

Resonance and synchronisation phenomena are observed in a variety of natural systems, ranging from biology [3, 4] to glacial cycles [5, 6]. Also, various physical systems, such as lasers [7, 8], electronic circuits [9] and mechanical pendulums [10] have been studied in this framework. Though externally forced and coupled oscillators have been studied extensively throughout the last century, some confusion between resonance and synchronisation exists in the literature [11].

Identifying the characteristic properties as well as differences between the phenomenon of resonance and that of synchronisation has several advantages to studying nonlinear dynamics of oscillating complex systems. It can be a valuable tool in construction of simplified models that capture the essential nonlinearities and are more amenable to analysis, thus allowing for an understanding of the underlying physical mechanisms. It can also provide valuable guidance in the analysis of complex systems (e.g. climate) where the detailed dynamics is often unknown and must be inferred from observations. Here, it can help enlighten the underlying mechanisms behind, say, a change in the observed oscillation frequency without any change in the forcing. In situations where the system cannot be separated from the forcing (e.g. climate paced by astronomical forcing) it can help answer questions about the intrinsic dynamics of the unforced system and the origin of oscillations. What is more, there are systems (e.g. lasers) where damped oscillations occur on top of self-sustained oscillations (e.g. stable limit

cycle with a pair of complex conjugate Floquet multipliers). Such systems exhibit responses to external forcing that are much more complex than nonlinear resonances or synchronisation alone [7, 21]. Identifying the characteristics of resonance, of synchronisation and of the interplay between these two phenomena can provide a valuable insight into nonlinear dynamics of such systems.

Whereas recent research has focused on nonlinear oscillators forced by irregular external signals, there are aspects of classical periodic forcing that have not been fully explored. Here, we shall concentrate on a detailed exploration of the paradigm of a damped nonlinear oscillator with periodic forcing

$$\frac{d^2x}{dt^2} + \gamma(x)\frac{dx}{dt} + x + x^3 = A \cos(\omega t), \quad (1.1)$$

where  $\gamma(x)$  is the normalised damping rate,  $A$  is the forcing strength,  $\omega$  is the normalised external forcing frequency, and the cubic nonlinearity  $x^3$  accounts for strong dependence of the natural frequency on the oscillation amplitude. Much of the analysis focuses on the damped Duffing oscillator, which is obtained by setting  $\gamma(x) = \gamma > 0$  in Eq. (1.1). In order to define synchronisation, we will also consider a generalisation of the damped Duffing oscillator to the self-sustained Duffing-Van der Pol oscillator with the sign-changing  $\gamma(x) = \gamma(x^2 - 1)$ , which acts as a source of energy into the system when  $|x| < 1$ .

In this paper, we relate resonance and synchronisation to the mathematical concept of bifurcations, and describe the main differences between characteristic properties of the two phenomena. Using bifurcation analysis, we uncover a novel resonance type which forms the backbone of the stability diagram but is unusual in the sense that it has (i) some of the characteristic properties of synchronised oscillations, and (ii) other properties that are unlike classical nonlinear resonances or synchronisation. What is more, we reinterpret the “intermingled tongues” defined from numerical simulations in [11], and link them to seemingly unrelated results on instabilities and chaos due to “bifurcation superstructure” in [1]. We obtain our main results for an intermediate damping strength  $\gamma = 0.01$ , and use bifurcation continuation techniques [12] to calculate the structure of resonance tongues in the parameter plane of the forcing frequency  $\omega$  and amplitude  $A$ .

### Bifurcation Superstructure: Odd and Even Resonances

Due to the nonlinear term  $x^3$ , which gives rise to amplitude-dependent natural frequency, Eq (1.1) with  $\gamma(x) = \gamma > 0$  exhibits many more resonances in addition to the main harmonic resonance near  $\omega = 1$ . For sufficiently small  $A$  and  $\gamma$ , these resonances occur near

$\omega = 1/k$ . They were first examined in detail by Parlitz and Lauterborn [1] (PL85), who refer to a resonance as odd (even) when  $k$  is odd (even). When  $A$  is increased, the resonances shift away from  $\omega = 1/k$  due to the forcing-induced change in the oscillation amplitude and the resulting shift in the corresponding natural frequency. (PL85) focus on moderate damping rate  $\gamma = 0.2$  and high forcing strength  $0 < A < 50$ , and perform numerical bifurcation analysis which reveals self-similar set of bifurcations with regions of chaos in the  $(\omega, A)$  parameter plane. They refer to the self-similar bifurcation set as “bifurcation superstructure”, and associate it with the alternating odd and even resonances.

### Intermingled Tongues

Paar and Pavin [11] (PP98) discuss coexisting attractors in Eq. (1.1) with weak damping  $\gamma(x) = \gamma = 0.001$  and moderate forcing strength  $0 < A < 5$ , using numerical simulations. This parameter range is devoid of bifurcations giving rise to chaotic oscillations. Instead, (PP98) demonstrate a high degree of multistability between periodic solutions and show an intriguing pattern of intermingled tongues in the  $(\omega, A)$  parameter plane. This pattern is shown in Fig. 1 which was obtained in the same way as [11, Fig.1] but for  $\gamma = 0.01$ , with different colours denoting different integer ratios of the period of periodic responses and the period  $2\pi/\omega$  of the forcing. However, unlike the “bifurcation superstructure” in (PL85), the pattern in (PP98) cannot be explained in terms of even and odd resonances, and it is referred to by (PP98) as “intermingled Arnold tongues”.

A comparison between (PL85) and (PP98) raises two questions. Firstly, it is unclear how Arnold tongues—a property of a dissipative self-sustained oscillator—can appear in a damped oscillator. Secondly, there is no indication whatsoever of any links between the “bifurcation superstructure” in (PL85) and “intermingled Arnold tongues” in (PP98). In the following analysis we show that the backbone of the intriguing pattern of intermingled tongues from (PP98) is formed by resonance tongues associated with the novel resonance type and not by Arnold tongues. Furthermore, we continue the largest resonance tongue of the novel type from  $\gamma = 0.01$  to  $\gamma = 0.2$ , and link it directly to an element of the “bifurcation superstructure” from (PL85).

### RESONANCE VS. SYNCHRONISATION

In order to illustrate the main differences between the phenomenon of resonance and the phenomenon of synchronisation, we compare in Fig. 2 the structure of the solutions to the damped and forced Duffing oscillator with  $\gamma(x) = \gamma = 0.01$  in panels (a) and (c), and the self-



sustained and forced Duffing-Van der Pol oscillator (1.1) with  $\gamma(x) = (x^2 - 1)\gamma$  in panels (b) and (d). Following are definitions and the listing of the characteristic properties for the two phenomena.

### Resonance

We define *resonance* phenomenon for a *linear or non-linear damped oscillator* as a noticeably increased amplitude of periodic oscillations near certain forcing frequencies.

The phenomenon is best illustrated by fixing  $A$  and plotting the *resonance curve*: the amplitude  $x_{max}$  of periodic solutions as a function of the forcing frequency  $\omega$ . Classical resonance in damped oscillators has the following characteristic properties:

- (r1) In a damped linear (harmonic) oscillator, there is only one resonance near the natural frequency. In a damped nonlinear oscillator, *depending on the type of nonlinearity in the last term on the l.h.s. of Eq (1.1)*, there will be additional *subharmonic resonances* when the forcing frequency approaches a fraction or a multiple of the natural frequency [13].
- (r2) For low to moderate forcing strength, the frequency of resonant response is the same as the forcing frequency. However, for larger  $A$ , the resonant response can be at a fraction of the forcing and natural frequencies, as demonstrated in the next Section. The frequency of periodic non-resonant response is the same as the forcing frequency.
- (r3) An onset of resonance, that is an increase in the amplitude of periodic oscillations as the forcing parameters are varied, *can be either quantitative or qualitative. In some oscillators (e.g. in a damped linear oscillator), the oscillation amplitude may increase gradually without any bifurcations or bistability. However, the majority of real-world oscillators have nonlinearities that give rise to amplitude-dependent natural frequency.* In such oscillators, the onset of resonance will involve bistability and qualitative changes in the dynamics, namely saddle-node or pitchfork bifurcations of periodic solutions.

For example, Fig. 2(a) shows the resonance curve for the Duffing oscillator with  $A = 0.05$  near the main resonance. The resonance curve ‘leans over’ so that there is a range of frequencies with two stable periodic solutions (solid branches), one of which has a much larger amplitude and corresponds to a resonant response; the two solutions also have different phases. Which of these two solutions the system settles to depends on initial conditions. This bistable range is bounded by two saddle-node

bifurcations  $SN$  of periodic solutions [14], marked with red diamonds in Fig. 2(a). By varying the amplitude and the frequency of the forcing, we have:

- (r4) In the  $(\omega, A)$  parameter plane, the corresponding codimension-one saddle-node or pitchfork bifurcation curves form *resonance tongues*. A resonance tongue has a tip for  $A$  small but nonzero and  $\omega$  near the natural frequency or near a fraction/multiple of the natural frequency. Moreover, the tip of an odd resonance tongue corresponds to a codimension-two cusp bifurcation  $C$  [14], where the two branches of the saddle-node bifurcation curve meet in a tangency [Fig. 2(c)]. Subharmonic resonance tongues appear for larger  $A$  than the harmonic resonance tongue [1].

Resonance tongues occur for sufficiently large  $A$  in damped nonlinear oscillators, where the system nonlinearities give rise to amplitude-dependent natural frequency. As  $A$  increases, resonance tongues shift in frequency, may overlap, develop additional cusp points, and interact with other bifurcations via special codimension-two bifurcation points, giving rise to complicated dynamics [1]. Note that overlapping resonance tongues indicate multistability. However, resonance is no longer defined for non-periodic oscillations arising at very large  $A$ . On the other hand, for values of  $A$  below the cusp point  $C$ , the corresponding resonance in a damped nonlinear oscillator does not show any bistability: locally, the resonance curve closely resembles the resonance curve of a damped linear (harmonic) oscillator.

### Synchronisation

We define *m:n synchronisation* phenomenon for  $m, n \in \mathbb{N}$  and a *dissipative self-sustained oscillator* as a stable and fixed-in-time relationship between the phases of the forcing  $\phi(t) = \omega t$  and of the oscillator  $\varphi(t)$ :

$$0 < |m\phi(t) - n\varphi(t)| \leq 2\pi \Rightarrow \frac{\omega}{\Omega} = \frac{n}{m},$$

where  $\Omega$  is the frequency of synchronised oscillations.

Classical synchronisation to periodic forcing has the following characteristic properties:

- (s1) A dissipative self-sustained oscillator can synchronise or phase-lock to periodic external forcing at various forcing frequencies provided that  $m\omega/n$  is sufficiently close to the natural frequency. Phase-locking is an important difference between the characteristic properties of resonance and synchronisation. Whereas a dissipative self-sustained oscillator can be phase-locked to oscillate near its natural frequency by forcing at a rational fraction of the

natural frequency, a damped oscillator cannot oscillate near its natural frequency when forced at a fraction of its natural frequency.

- (s2) The frequency of the periodic synchronised response is  $\Omega = m\omega/n$ , which by (s1) is close to the natural frequency. However, unsynchronised response is quasiperiodic or chaotic.

Fig. 2(b) shows a range of forcing frequencies where the oscillator (1.1) synchronises in the ratio 1:1 to periodic external forcing. The solid curve is a branch of stable periodic solutions corresponding to the synchronised response, while the dashed curve is a branch of unstable periodic solutions. The two branches meet and disappear in a saddle-node bifurcation of periodic solutions at both ends of the 1:1 synchronisation range [red diamonds in Fig. 2(b)]. On each side of the 1:1 synchronisation range, there are disconnected dots. In the dotted area, there are two types of solutions that are difficult to distinguish in the diagram: unsynchronised quasiperiodic solutions due to incommensurate ratio of the oscillator frequency and the forcing frequency are interspersed with narrow ranges of higher-period synchronised solutions. Although resonances and synchronisation may involve the same bifurcation type, there are important differences between these two nonlinear phenomena:

- (s3) A synchronisation-desynchronisation transition is always a qualitative phenomenon that corresponds to saddle-node bifurcation  $SN$  of periodic solutions [Fig. 2(b)]. What is more, there is no bistability of periodic solutions at low to moderate  $A$ , which is in stark contrast to nonlinear resonances.
- (s4) In the  $(\omega, A)$  parameter plane, the corresponding saddle-node bifurcation curves form  $m:n$  synchronisation tongues or *Arnold tongues* [15, 16]; see Fig. 2(d) for an example of a 1:1 synchronisation tongue in the Duffing-Van der Pol oscillator (1.1). In contrast to a resonance tongue, a  $m:n$  synchronisation tongue has a tip at  $A = 0$  and  $\omega = n\omega_0/m$ , where  $\omega_0$  is the frequency of the self-sustained oscillations. Another difference from an odd resonance tongue is that the tip of an Arnold tongue is not a cusp bifurcation.

The synchronisation phenomenon is captured in the  $(\omega, A)$  parameter plane by an infinite but countable number of Arnold tongues. Unlike resonance tongues, Arnold tongues originate at  $A = 0$  and  $\omega = n\omega_0/m$ , where  $m, n \in \mathbb{N}$ . As  $A$  is increased, the tongues widen and may shift in frequency but they do not overlap until some critical value of  $A_c > 0$ . Above  $A_c$ , overlapping tongues indicate break-up of invariant tori through various mechanisms including homoclinic tangencies between stable

and unstable manifolds of saddle-type periodic solutions like the one indicated with a dashed curve in Fig. 2(b), giving rise to chaotic oscillations [17, 18]. The model example of Arnold tongues is the circle map [15, 19].

The remainder of this paper focuses on a novel type of a nonlinear resonance in the Duffing oscillator, which explains the pattern of intermingled tongues in (PP98) and links it to the “bifurcation superstructure” in (PL85).

### COMPLICATED RESONANCE CURVE: THREE RESONANCE TYPES

To explain the high degree of multistability and the structure of intermingled tongues observed in numerical simulations, we analyse the resonance structure in Eq. (1.1) with  $\gamma(x) = \gamma = 0.01$  using two different techniques. On the one hand, *bifurcation diagrams* are obtained using numerical continuation techniques AUTO [12], which allow parameter continuation of stable and unstable periodic solutions and their bifurcations. On the other hand, *attractor diagrams* are obtained by direct time integration of Eq. (1.1).

#### Conventional Resonances

Besides the harmonic resonance depicted in Fig. 2(a), there are subharmonic resonances in accordance with property (r1). The resonance curve in Fig. 3 obtained by continuation shows that subharmonic resonances occur for  $\omega < 1$  and become distinct only for larger  $A$  than the one used in Fig. 2(a). In Fig. 3, we use  $A = 3$  and adopt notation from (PL85) denoting a (subharmonic) resonance occurring near  $\omega = (\text{natural frequency})/k$  with  $R_k$ .

In Fig. 3(a) we zoom in on the subharmonic resonances. Here it is seen that parts of the resonance curve are ‘punctuated’ by intervals of unstable periodic solutions. There are two types of punctuation. Firstly, in the odd resonances ( $k > 1$  and odd), the stable and unstable solutions merge in saddle-node bifurcations  $SN$  (diamonds in Fig. 3(a)). Secondly, the unstable solutions found between the odd resonances are bounded by pairs of pitchfork bifurcations  $P$  (squares in Fig. 3(a)). These bifurcations give rise to pairs of stable symmetry-broken periodic solutions, shown in red in Fig. 3(b), which appear as mirror imaged orbits  $x \leftrightarrow -x$  in the  $(x, \dot{x})$  plane [insets in Fig. 3(b)] [1, 20]. These solutions correspond to even subharmonic resonances ( $k > 1$  and even) and become distinct for  $A$  larger than the odd subharmonic resonances. What is more, they themselves undergo saddle-node bifurcations giving rise to regions of multistability of symmetry-broken periodic solutions.

Both bifurcation types, that is  $SN$  and  $P$ , indicate qualitative changes in the solutions associated with (sub-

harmonic) resonances in accordance with property (r3). Interestingly, the odd and even resonances alone cannot explain the intermingled tongue structure from Fig. 1. This means that there must be additional nonlinear resonances due to periodic solutions that are not connected to the primary branch (black curve in Fig. 3).

### Isolated Resonances

Figure 4 shows a one-dimensional attractor diagram obtained for the same initial conditions  $(x(0), \dot{x}(0)) = (0, 0)$  for each value of  $\omega$ .<sup>1</sup> A comparison with the bifurcation diagram from Fig. 3(b) reveals stable periodic solutions that belong to stable branches of the resonance curve from Fig. 3(b), as well as additional stable periodic solutions that are not present in Fig. 3(b). These additional solutions are symmetric period-3 oscillations shown in Fig. 5. What is more, parameter continuation of these additional solutions reveals that they form “isolas” disconnected from the primary branch of periodic solutions (green branches are disconnected from the black and red branches in Fig. 6).

We have now in Figs. 3 and 6 identified three different resonance types. These include previously studied:

- (i) *odd resonances* which occur on the (black) branch of primary (symmetric) periodic solutions and oscillate at the forcing frequency, and
- (ii) *even resonances* due to (red) symmetry-broken periodic solutions which bifurcate off the primary branch and also oscillate at the forcing frequency, as well as uncovered here
- (iii) *isolated resonances* due to (green) isolas of periodic solutions with greatly increased amplitude of oscillations.

Isolated resonances are unusual for the following reasons. Firstly, the frequency of oscillation is a fraction of the forcing frequency, even though the forcing frequency is a fraction of the natural frequency. Such response is unlike odd and even resonances or synchronisation. Secondly, the periodic solutions involved are bounded by saddle-node bifurcations in a way that is reminiscent of characteristic properties of synchronisation in Fig. 2(b) rather than characteristic properties of nonlinear resonances in Fig. 2(a). As a consequence, cusp points at low  $A$  are not expected in the corresponding resonance tongues. Thirdly, isolated resonances give rise to a complicated and unusual resonance curve in Fig. 6, consisting of connected odd and even subharmonic resonances as well as disconnected components, which give rise to many regions of multistability.

<sup>1</sup> It may appear from Figure 4 that there are different attracting periodic orbits for the same value of  $\omega$  despite fixed initial conditions. This is not the case. Rather, the system sometimes converges to different periodic solutions for neighbouring values of  $\omega$ .

### The Onset and Termination of Resonances

We note that, as  $A$  is increased, the onset of odd resonances need not be clear-cut. More precisely, while the cusp point seems to be a good indicator for the onset of an odd resonance, there can be a noticeable uplift in the resonance curve already for values of  $A$  just below the cusp point. On the other hand, the onset of even resonances is a qualitative transition associated with appearance of pairs of pitchfork bifurcations. Similar is true for isolated resonances, whose onset is a qualitative transition associated with appearance of pairs of saddle-node bifurcations. Hence, the onset of even and isolated resonances is clear-cut and can be defined properly. Furthermore, as parameters are varied, there can be other bifurcations, past which all three types of nonlinear resonances may become difficult to distinguish or even difficult to define (e.g. non-periodic oscillations). For example, for sufficiently large  $A$ , branches of periodic solutions belonging to even and odd resonances may develop additional connections, other than through the (black) branch of primary periodic solutions, so that one can no longer clearly distinguish between the two types of resonances. Similarly, it is possible for isolated resonances to connect to other branches of periodic solutions and cease to be isolated; see the next Section. However, such transitions would require qualitative changes (bifurcations). Thus, it should be possible to pin down termination points for all three resonance types.

### RESONANCE TONGUES

The three resonance types in the complicated resonance curve from Fig. 6 can be characterised and studied in terms of saddle-node (diamonds) and pitchfork (squares) bifurcation points. In the two-dimensional  $(\omega, A)$  parameter plane, these bifurcations can be continued with AUTO to obtain the corresponding bifurcation curves which are referred to as resonance tongues [property (r4)]. Fig. 7 shows the resonance tongues computed for all three types of resonances. These include: (black) saddle-node bifurcations of the primary branch of periodic solutions which correspond to odd subharmonic resonances, (red) pitchfork bifurcations on the primary branch of periodic solutions which correspond to even subharmonic resonances, (blue) saddle-node bifurcations of the symmetry-broken periodic solutions which give rise to multistability of even resonances, and (green) saddle-node bifurcations bounding the isolas which correspond to isolated resonances.

### Explaining the “intermingled tongue structure”

The structure of the resonance tongues bears strong resemblance to the “intermingled Arnold tongues” reported by (PP98) (Fig. 1). We can now superimpose the periodic solutions oscillating at various fractions of the forcing frequency from Fig. 1 obtained by direct time integration over the resonance tongues from Fig. 7 obtained by continuation. The resulting Fig. 8 reveals perfect match between the (green) resonance tongues corresponding to the isolated resonances and (red) regions with stable periodic solutions oscillating at a third of the forcing frequency. Thus, the intriguing patchy tongue structure found in (PP98) and shown in Fig. 1 can be identified with the isolated resonances, which appear to form the backbone of the structure. Furthermore, the patchiness of the tongues is a result of multistability: there are multiple stable periodic solutions of different period for the same parameter settings and, as the initial conditions are fixed but the parameters  $\omega$  and  $A$  are varied, the system can settle to a different periodic solution.

There are additional isolated resonances with stable periodic solutions oscillating at  $\omega/n$  for  $n = 2, 4, 5, \dots$ , whose resonance tongues match the remaining patchy tongues from Fig. 1. For clarity, these additional isolated resonance tongues are left out in Fig. 8.

### Links to “bifurcation superstructure”

Our analysis of the intermediate damping rate  $\gamma = 0.01$  and moderate forcing strength  $0 < A < 6$  reveals various periodic solutions and their bifurcations. However, we have not found any bifurcations, such as torus bifurcations or period-doubling cascades, that would eventually lead to irregular or chaotic oscillations. Rather, the saddle-node and pitchfork bifurcations give rise to regions of multistability of periodic solutions.

As the damping rate  $\gamma$  is decreased, the patchy tongues become more abundant. This was demonstrated by (PP98) for  $\gamma = 0.001$ . Hence, isolated resonances become even more prominent at low damping, where they appear at even lower  $A$  and give rise to a greater degree of multistability of periodic solutions.

On the other hand, as the damping rate is increased, isolated resonances seem to give way to the “bifurcation superstructure” involving period-doubling cascades, period-3 solutions and chaotic attractors, which were reported for  $\gamma = 0.2$  and  $10 < A < 50$  by (PL85).

An interesting question emerges whether isolated resonances are purely a low-damping phenomenon or whether the period-3 solutions associated with isolated resonances (Fig. 5) are related to the “bifurcation superstructure” from [1]. To address this question we continued the largest isolated resonance tongue from Fig. 7 to higher values of  $\gamma$ . The results of the continuation are shown in

Fig. 9. As  $\gamma$  is increased from  $\gamma = 0.01$  [Fig. 9(a)], the isolated resonance tongue moves to higher values of  $A$  and develops another tip [Fig. 9(b-c)]. At  $\gamma = 0.2$  the continuation of the isolated resonance tongue matches exactly an element of the “bifurcation superstructure” denoted with  $R_{9,3}$  in [1, Fig.6]. Thus, in addition to explaining “intermingled tongues”, isolated resonances: (i) provide a link between “intermingled tongues” the “bifurcation superstructure”, and (ii) give new insight into “bifurcation superstructure” which now appears to be organised by three rather than two different resonance types.

The key difference between the weak and moderate damping is that periodic solutions involved in isolated resonances at low  $\gamma$  may cease to be isolated as  $\gamma$  is increased. The bifurcation diagram in Fig. 10(a) for  $\gamma = 0.2$ ,  $A = 25$  and  $1.15 \leq \omega \leq 1.7$ , shows the primary branch of periodic solutions (black), the symmetry-broken solutions bifurcating off the primary branch (red) via pitchfork bifurcation (square), two potentially isolated components of periodic solutions (green), and symmetry-broken solutions (blue) bifurcating from the left potentially isolated component via pitchfork bifurcation (square). In Fig. 10(b), *attractor diagram obtained by starting on the stable branch of each (green) potentially isolated component is superimposed over the bifurcation diagram from panel (a)*. The right-hand side component turns out to be isolated. However, the larger left-hand side component turns out to be connected to other stable solutions. Starting at the stable periodic solution of this component and decreasing  $\omega$ , the solution loses stability via symmetry-breaking pitchfork bifurcation, then the symmetry-broken solution undergoes period-doubling cascade to chaos, followed by an inverse period-doubling cascade to (red) period-one solution which, in turn, connects to (black) the primary branch of periodic solutions via pitchfork bifurcation.

### CONCLUSION

We have investigated nonlinear resonances of a periodically forced Duffing oscillator. We have identified novel isolated resonances in addition to already known odd and even subharmonic resonances, and demonstrated a complicated resonance ‘curve’ with isolas (isolated components) of periodic solutions and high degree of multistability. Most importantly, the identified here isolated resonances in conjunction with numerical continuation techniques allowed us to (i) explain and reinterpret the intriguing structure of “intermingled tongues” observed in stability diagrams for weak damping and (ii) link those “intermingled tongues” to a seemingly unrelated phenomenon of “bifurcation superstructure” found for moderate damping.

Firstly, to avoid confusion between resonance and synchronisation, we defined each phenomenon and gave a



short discussion of their characteristic properties and the key differences. We also described how the two phenomena exhibit themselves in the stability diagrams. In particular, we distinguished between resonance tongues and synchronisation tongues, which are also known as Arnold tongues, in the parameter plane of the forcing frequency vs. the forcing amplitude. Secondly, we have shown that resonance tongues associated with the isolated resonances form the backbone of the intriguing pattern of “intermingled tongues” at weak damping, which were reported by Paar and Pavin and mistaken for Arnold tongues [11]. Thirdly, we have demonstrated that, as the damping rate increases, isolated resonances may bifurcate and cease to be isolated. As a result of such bifurcations, the corresponding resonance tongues become particular elements of the “bifurcation superstructure” reported by Parlitz and Lauterborn for moderate damping [1].

The new insight into nonlinear resonances in the simple Duffing oscillator can be extended to more complicated systems. One example are class-B lasers which exhibit damped oscillations (relaxation oscillation onto the lasing solution) and self-sustained oscillations (the lasing solution itself) at the same time. Stability diagrams for lasers subject to external optical injection [21, Figs. 9-11] show variety of coexisting tongues, which can be interpreted as a combination of a 1:1 synchronisation tongue and different types of nonlinear resonance tongues.

The distinction between the phenomenon of resonance and that of synchronisation is highly relevant in forced complex systems (e.g. climate) where the detailed internal dynamics is unknown and inferences are made from observations. The prime example in climate science is the phenomenon of ice ages, that is, a series of glacial events separated by interglacial events [22]. There is evidence that ice age cycles are linked to variations in the Earth’s orbit; however, the actual type of relationship between the frequencies observed in the paleoclimatic records and those present in the orbital forcing has not been identified to date [5, 6].

Physics Reports **416**, 1 (2005).

- [1] U. Parlitz and W. Lauterborn, *Physics Letters A* **107**, 351 (1985).
- [2] A. Pikovsky, M. Rosenblum, and J. Kurths, *Synchronization: a universal concept in nonlinear sciences*, Vol. 12 (Cambridge university press, 2003).
- [3] R. FitzHugh, *Biophysics J* **1**, 445 (1961).
- [4] J. Nagumo, S. Arimoto, and S. Yoshizawa, *Proceedings of the IRE* **50**, 2061 (1962).
- [5] M. Crucifix, *Philosophical Transactions of the Royal Society of London A: Mathematical, Physical and Engineering Sciences* **370**, 1140 (2012).
- [6] B. De Saedeleer, M. Crucifix, and S. Wiczeorek, *Climate Dynamics* **40**, 273 (2013).
- [7] S. Wiczeorek, B. Krauskopf, T. Simpson, and D. Lenstra,

- [8] M. C. Soriano, J. García-Ojalvo, C. R. Mirasso, and I. Fischer, *Reviews of Modern Physics* **85**, 421 (2013).
- [9] B. Van der Pol, *The London, Edinburgh, and Dublin Philosophical Magazine and Journal of Science* **2**, 978 (1926).
- [10] G. Duffing, *Erzwungene Schwingungen bei veränderlicher Eigenfrequenz (Forced vibration with variable natural frequency)*, Vol. 41/42 (F. Vieweg, Braunschweig, 1918).
- [11] V. Paar and N. Pavin, *Phys. Rev. E* **57**, 1544 (1998).
- [12] E. Doedel and B. Oldeman, “Auto-07p: Continuation and bifurcation software for ordinary differential equations. concordia university,” (2009).
- [13] W. Lauterborn, *The Journal of the Acoustical Society of America* **59**, 283 (1976).
- [14] Y. A. Kuznetsov, *Elements of applied bifurcation theory* (Springer, 1998).
- [15] P. L. Boyland, *Comm. Math. Phys.* **106**, 353 (1986).
- [16] J. Norris, *Nonlinearity* **6**, 1093 (1993).
- [17] S. Ostlund, D. Rand, J. Sethna, and E. Siggia, *Physica D: Nonlinear Phenomena* **8**, 303 (1983).
- [18] H. Broer, C. Simó, and J. C. Tatjer, *Nonlinearity* **11**, 667 (1998).
- [19] E. Ott, *Chaos in dynamical systems* (Cambridge university press, 2002).
- [20] P. Holmes, *Philosophical Transactions of the Royal Society of London A: Mathematical, Physical and Engineering Sciences* **292**, 419 (1979).
- [21] B. Krauskopf and S. Wiczeorek, *Physica D: Nonlinear Phenomena* **173**, 97 (2002).
- [22] L. E. Lisiecki and M. E. Raymo, *Paleoceanography* **20** (2005).

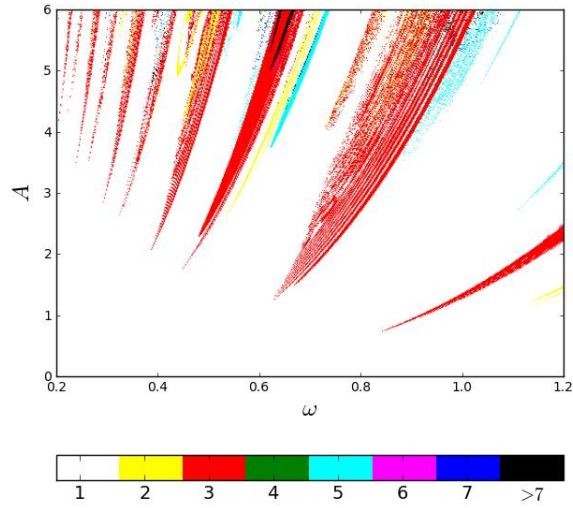


**Figure 1:** Two-dimensional attractor diagram in the  $(\omega, A)$  parameter plane indicating regions with stable periodic orbits of the forced Duffing oscillator (Eq. (1.1) with  $\gamma(x) = \gamma = 0.01$ ) of frequency (blank)  $\omega$ , (yellow)  $\omega/2$ , (red)  $\omega/3$ , (green)  $\omega/4$ , (cyan)  $\omega/5$ , (magenta)  $\omega/6$ , (blue)  $\omega/7$ , and (black)  $\omega/n$  for  $n = 8, 9, \dots$ . We used fixed initial conditions  $x(0) = \dot{x}(0) = 0$ .



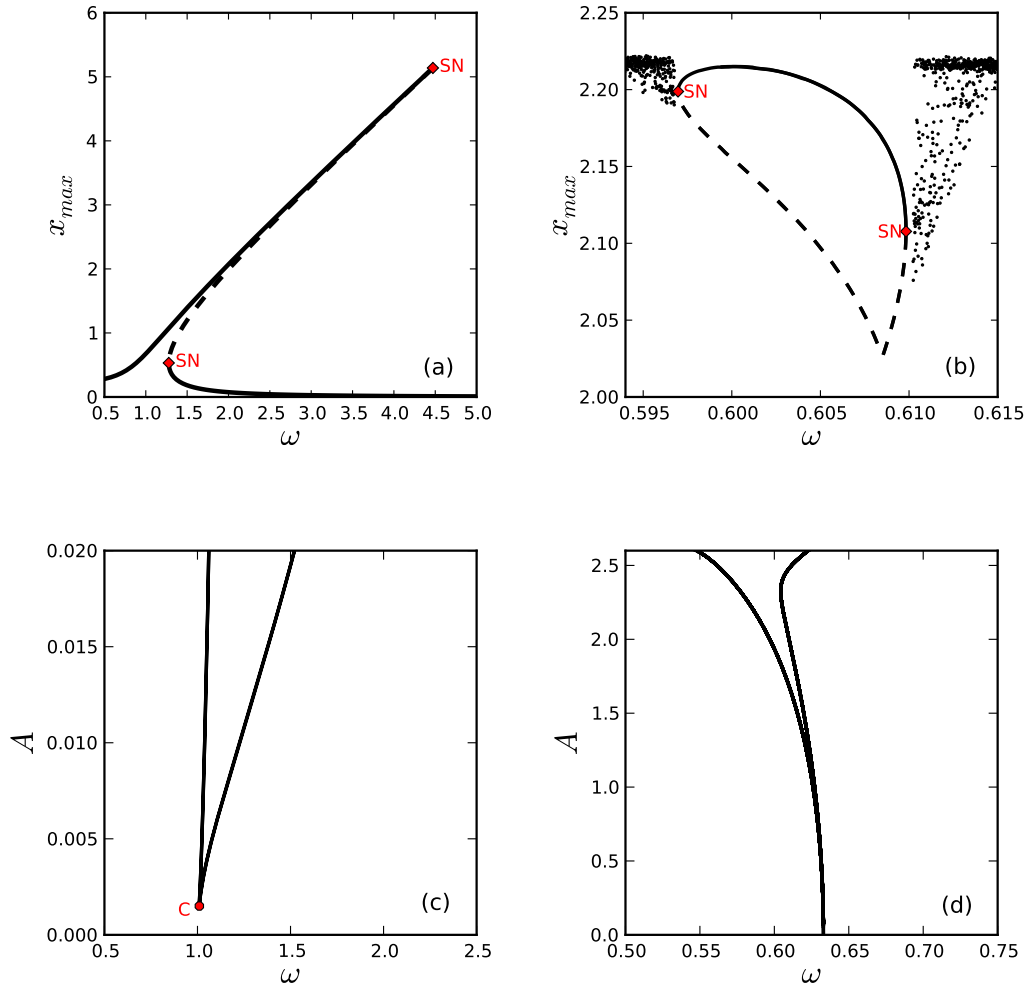


**Figure 2:** (a) One-dimensional bifurcation diagram showing the resonance curve near the primary resonance of the forced Duffing oscillator (Eq. (1.1) with  $\gamma(x) = \gamma = 0.01$ ). The black solid curves mark the stable solutions, the black dashed curve marks the unstable solutions. Saddle-node bifurcations (SN) are marked by the red diamonds. Fixed parameters and initial condition:  $A = 0.05$ ,  $\gamma = 0.01$ ;  $x(0) = 0$ ,  $\dot{x}(0) = 0$ . (b) Values of the maxima of  $x(t)$  as a function of  $\omega$  showing periodic and quasi-periodic oscillations of the Duffing-Van der Pol system (Eq (1.1) with  $\gamma(x) = \gamma(x^2 - 1)$ ). The black solid curve marks the stable periodic solution, the black dashed curve marks the unstable periodic solution. Outside the 1:1 synchronisation region, regions of quasiperiodic solutions are intermingled with narrow regions of higher-period periodic solutions (scattered black dots). Fixed parameters and initial condition:  $A = 2.0$ ,  $\gamma = 0.01$ ;  $x(0) = \dot{x}(0) = 0$ . (c) Two parameter continuation ( $\omega, A$ ) of the saddle-node bifurcations shown in panel (a). The cusp bifurcation  $C$ , where the two saddle-node bifurcations merge, is marked by the red circle. Note that the cusp occurs for  $A > 0$ . (d) Two parameter continuation ( $\omega, A$ ) of the saddle-node bifurcations shown in panel (b). Note that the tip of the tongue occurs for  $A = 0$  and is not a cusp bifurcation.

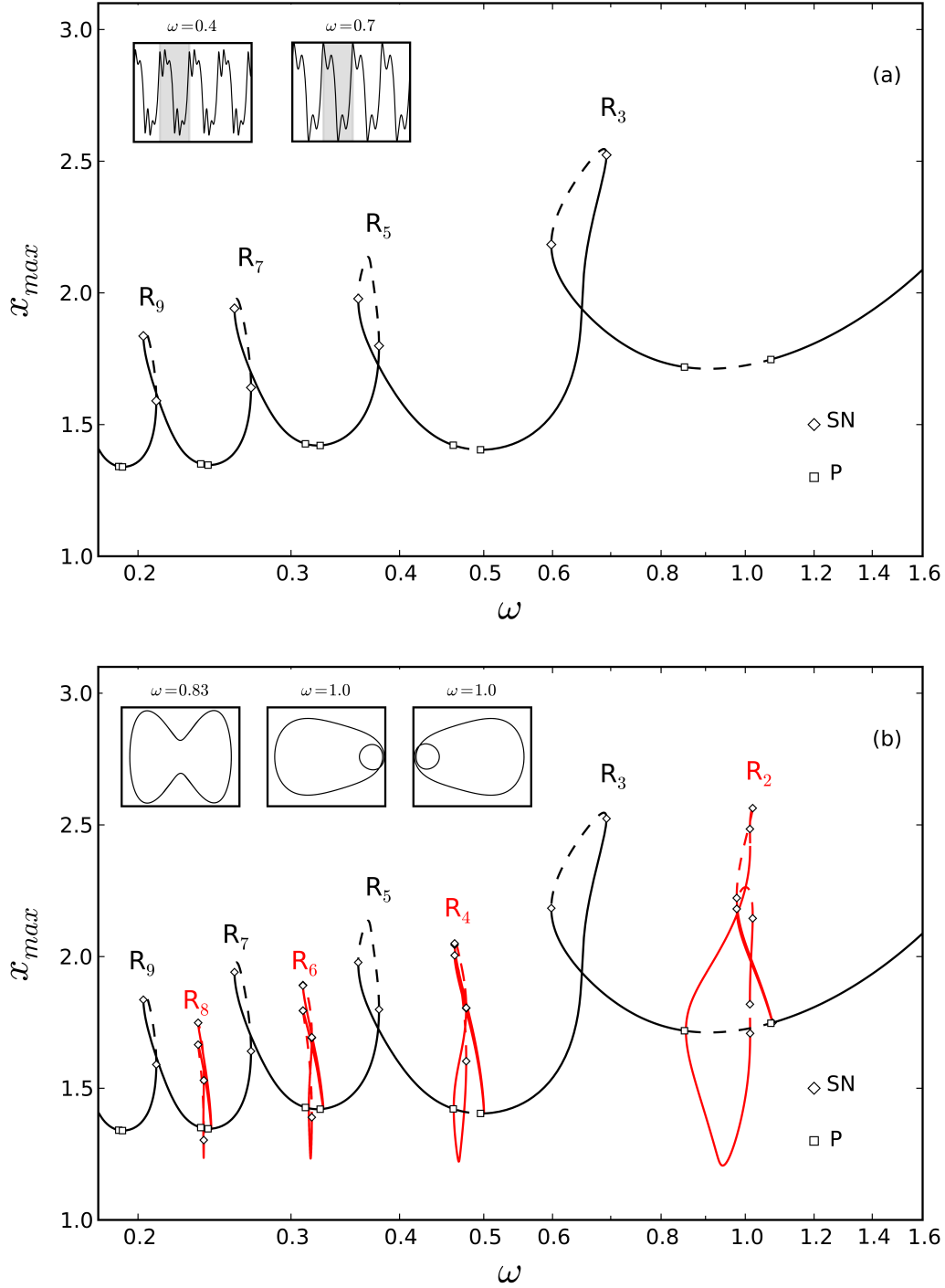


**Figure 3:** (a) Part of the resonance curve showing branches of periodic solutions as a function of the forcing frequency  $\omega$ . On the primary branch of symmetric periodic solutions (black curve), saddle-node bifurcations (diamonds) and pitchfork bifurcations (squares) take place. Stable branches are marked by solid curves, unstable branches by dashed curves. Fixed parameters:  $A = 3$ ,  $\gamma = 0.01$ . The inserts show two solutions in the  $(t, x)$  plane. For  $\omega = 0.4$  the solution is on the  $R_5$  branch, where there are 5 local maxima in one period, marked by the gray band. For  $\omega = 0.7$  the solution is on the  $R_3$  branch, where there are 3 local maxima in one period. (b) Same as (a), now including (red) even resonances in addition to odd resonances. At pitchfork bifurcations, pairs of stable symmetry-broken solutions appear. Inserts show stable periodic solutions in the  $(x, \dot{x})$ -phase plane just before ( $\omega = 0.83$ ), and just after the  $x \rightarrow -x$  symmetry breaking pitchfork bifurcation ( $\omega = 1.0$ ).

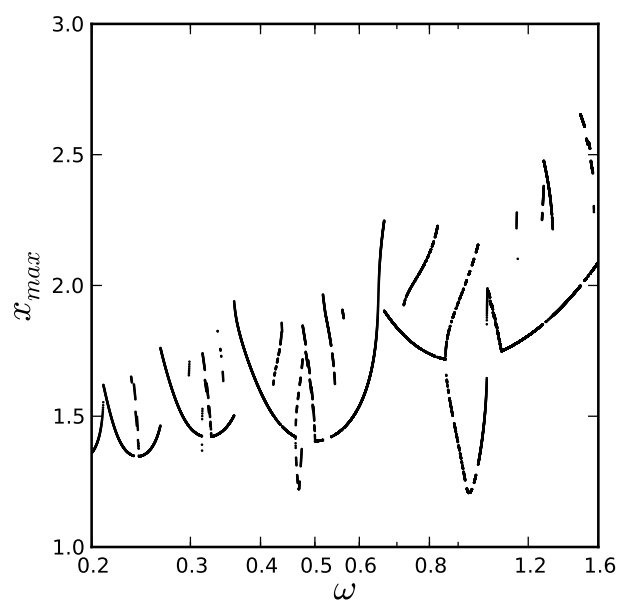


**Figure 4:** One-dimensional attractor diagram of the forced Duffing oscillator (Eq. (1.1) with  $\gamma(x) = \gamma = 0.01$ ) showing the maxima of  $x(t)$  plotted versus  $\omega$  for  $\gamma = 0.01$ ,  $A = 3$ ,  $x(0) = \dot{x}(0) = 0$ .

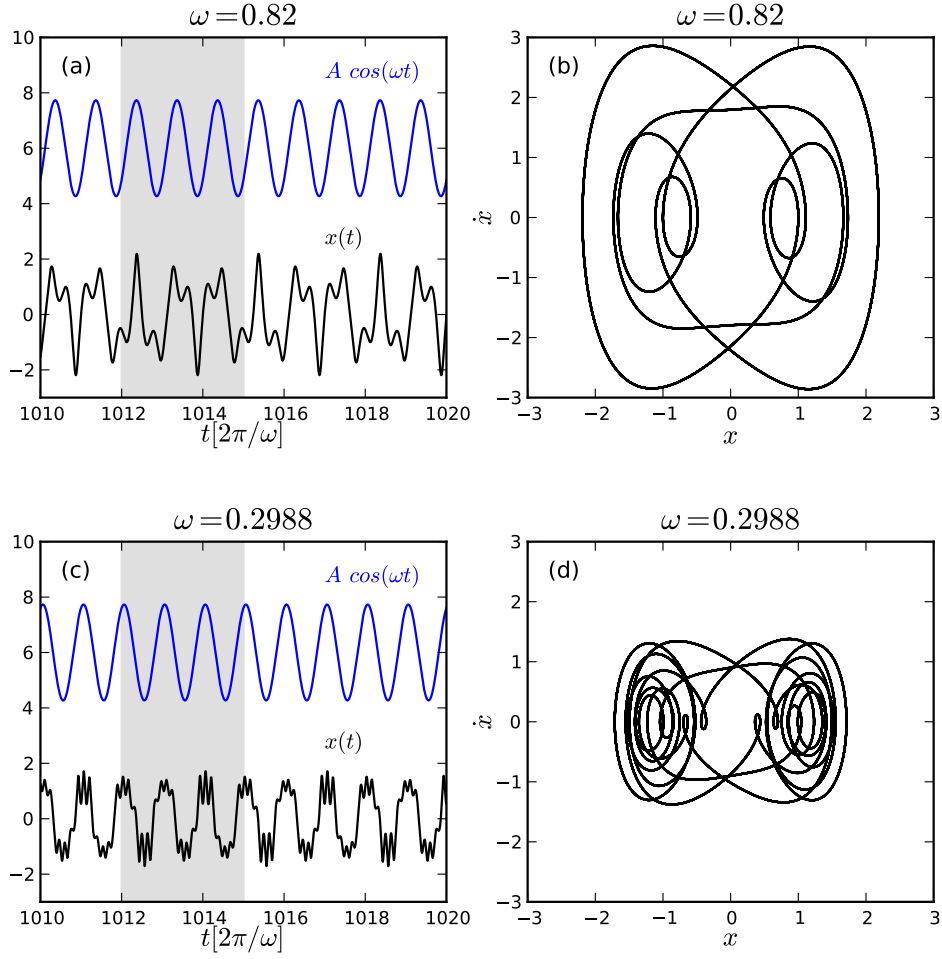


**Figure 5:** Equation (1.1) with  $\gamma(x) = \gamma = 0.01$  has been integrated over 1020 periods of the forcing. The additional attracting periodic orbits of the Duffing oscillator are shown for the last 10 periods of the forcing in the  $(t, x)$  and  $(x, \dot{x})$  planes. The solutions are period-3 orbits indicated by the gray bands. Fixed parameters and initial condition:  $A = 3$ ,  $\gamma = 0.01$ ,  $x(0) = \dot{x}(0) = 0$ . (a) Trajectory in the  $(t, x)$  plane,  $\omega = 0.82$ . (b) Phase portrait in the  $(x, \dot{x})$  phase plane,  $\omega = 0.82$ . (c) Trajectory in the  $(t, x)$  plane,  $\omega = 0.2988$ . (d) Phase portrait in the  $(x, \dot{x})$  phase plane,  $\omega = 0.2988$ .

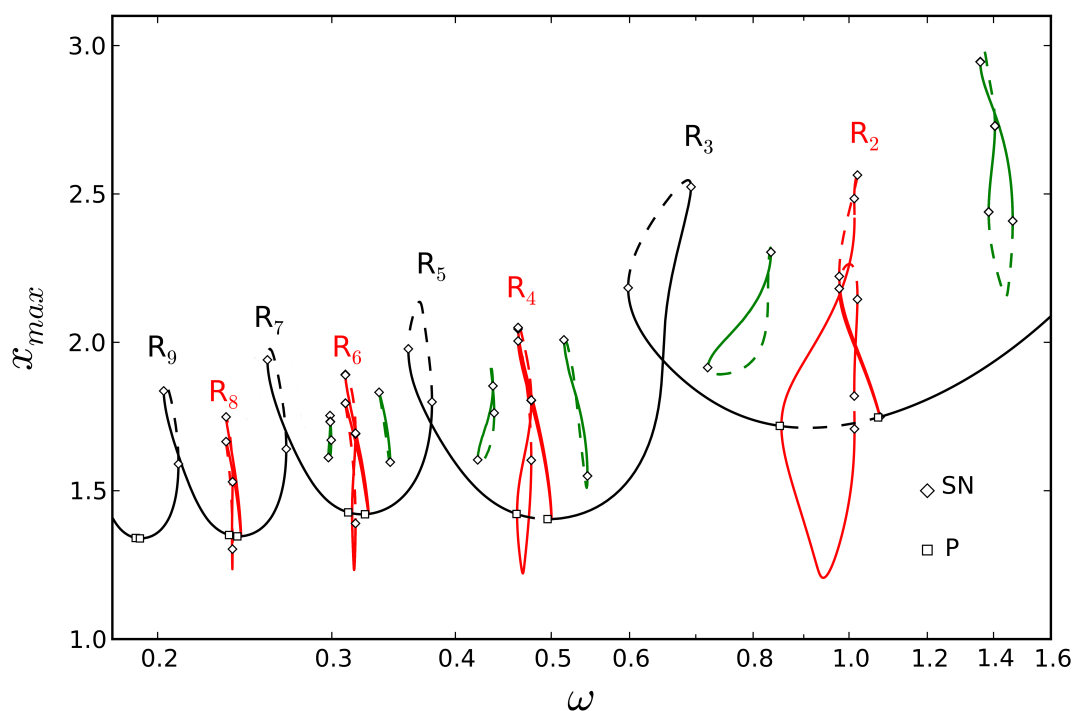


**Figure 6:** Same resonance curve as in Figure 3, but now showing three different types of resonances: (black curve) odd resonances occurring on the symmetric branch of periodic solutions, (red curves) even resonances occurring on the asymmetric branches of periodic solutions, and (green curves) isolated resonances. Stable branches are marked by solid curves and unstable branches are marked by dashed curves. Fixed parameters:  $A = 3$ ,  $\gamma = 0.01$ .

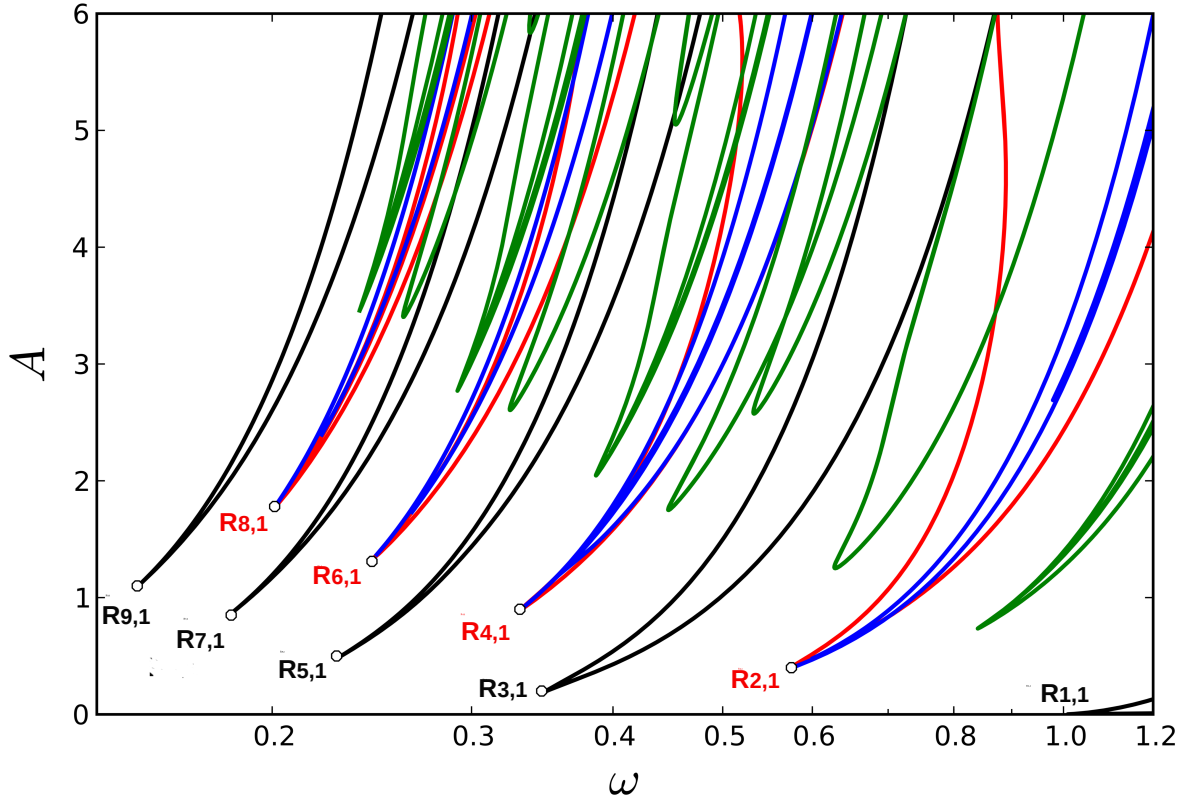


**Figure 7:** Two-dimensional bifurcation diagram in the  $(\omega, A)$  parameter plane showing all three types of resonance tongues computed as bifurcation curves. These include: (black) saddle-node bifurcations of the primary branch of periodic solutions which correspond to odd subharmonic resonances, (red) pitchfork bifurcations on the primary branch of periodic solutions which correspond to even subharmonic resonances, (blue) saddle-node bifurcations of the symmetry-broken periodic solutions which give rise to multistability of even resonances, and (green) saddle-node bifurcations bounding the isolas which correspond to isolated resonances. Using the notation adopted in (PL85), the resonance tongues computed for the resonance type (i) (*odd resonances*) are denoted by  $R_{1,1}$ ,  $R_{3,1}$ ,  $R_{5,1}$ ,  $R_{7,1}$ ,  $R_{9,1}$ , and the resonance tongues computed for the resonance type (ii) (*even resonances*) are denoted by  $R_{2,1}$ ,  $R_{4,1}$ ,  $R_{6,1}$ ,  $R_{8,1}$ . The first subscript indicates the winding number (here defined as the number of maxima or minima of the periodic solution in one period) and the second subscript is the period in unit of the forcing period  $2\pi/\omega$ . Fixed parameter:  $\gamma = 0.01$ . The open circles indicate cusp bifurcations.



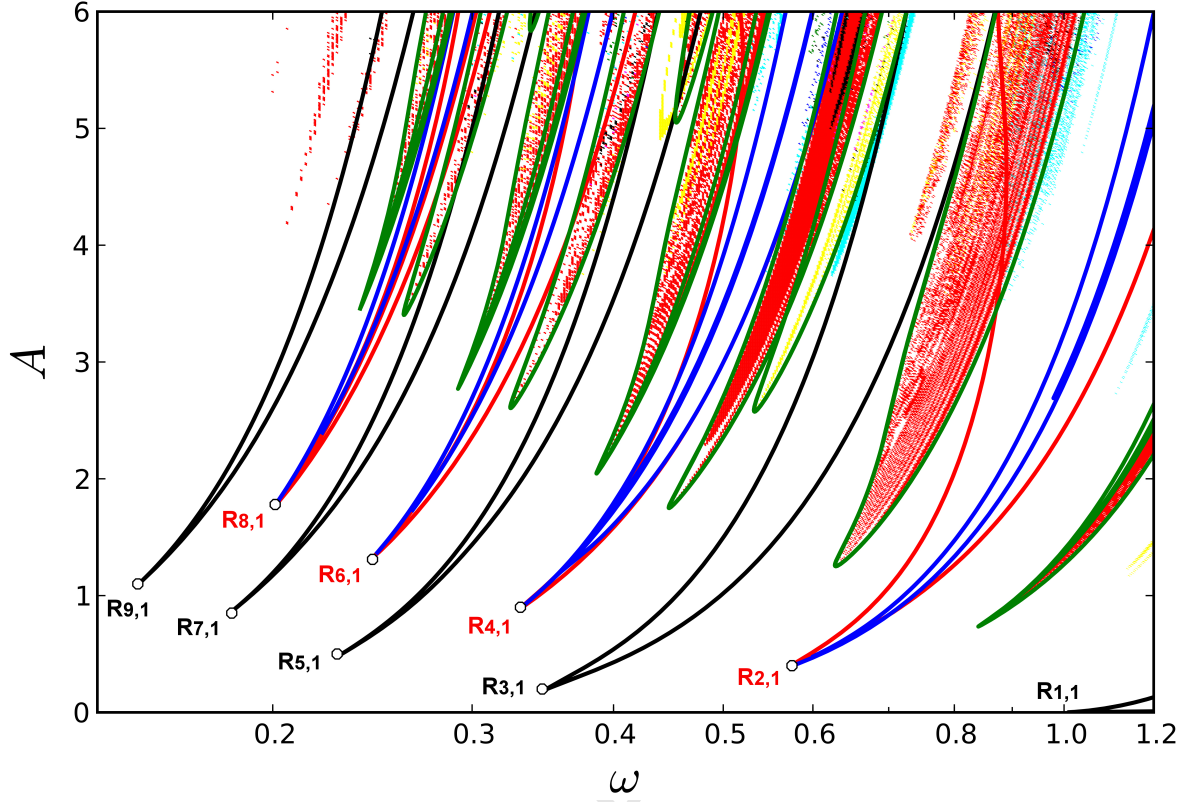


**Figure 8:** Two-dimensional attractor diagram in the  $(\omega, A)$  parameter plane showing regions with stable periodic solutions of period  $nT_F$ ,  $n = 1, \dots, 7$  (same as Fig. 1) is superimposed over two-dimensional bifurcation diagram showing all three types of resonance tongues (same as Fig. 7). The (red) regions with stable period-3 solutions and the (green) resonance tongues corresponding to the isolated resonances match perfectly. The open circles indicate cusp bifurcations.

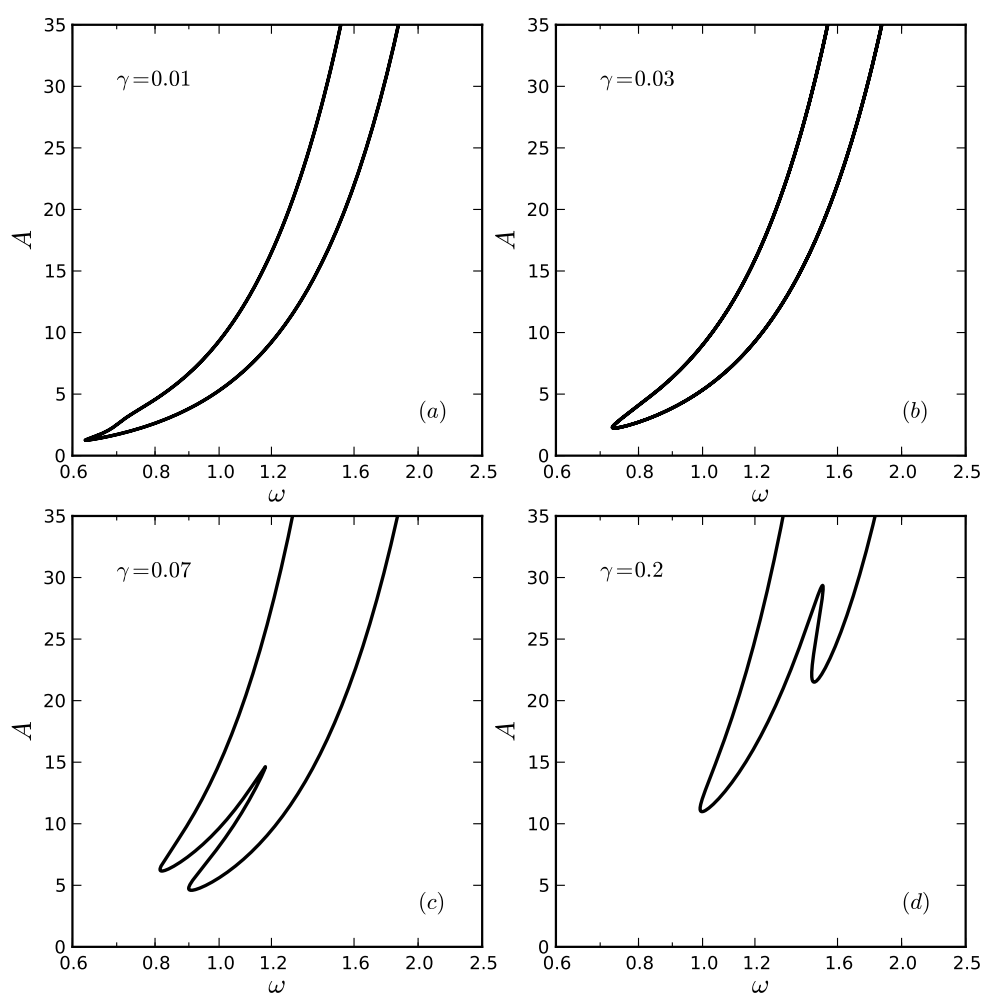


**Figure 9:** Saddle-node bifurcation curve corresponding to the largest isolated resonance tongue for different values of the damping parameter  $\gamma$ .

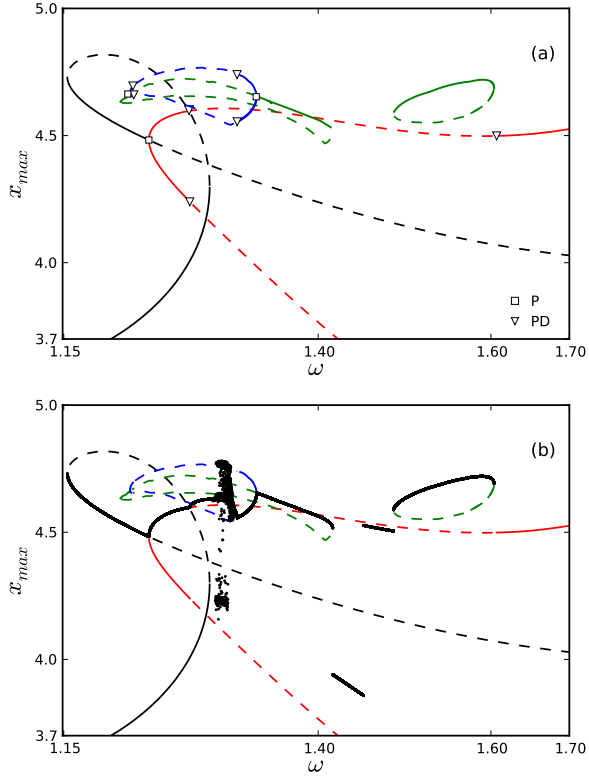


**Figure 10:** (a) One-dimensional bifurcation diagram in the range  $1.15 < \omega < 1.7$  showing (black) the primary branch of periodic solutions, (red) symmetry-broken solutions bifurcating off the primary branch, (green) isolas of periodic solutions, and (blue) symmetry-broken solutions bifurcating from the left isola. (b) One-dimensional attractor diagram (black dots) is superimposed over the bifurcation diagram from panel (a). The attractor diagram consists of four computation runs: starting at the centre of the (green) stable right and left isolas of periodic solutions, the control parameter  $\omega$  is increased and decreased.

- Forced nonlinear oscillators can exhibit unusual isolated resonances.
- Isolated resonances give rise to intricate resonance curves with isolated components.
- Isolated resonances provide a link between seemingly unrelated nonlinear phenomena.